energies

MDPI

Article

Series FACTS Devices for Increasing Resiliency in Severe Weather Conditions

Milad Beikbabaei and Ali Mehrizi-Sani *

The Bradley Department of Electrical and Computer Engineering, Virginia Polytechnic Institute and State University, Blacksburg, VA 24061, USA; miladb@vt.edu
* Correspondence: mehrizi@vt.edu

Abstract: Severe weather conditions are low-probability, high-impact events that affect grid operations. The majority of power outages are caused by severe weather conditions. Grid resiliency to weather events can be enhanced by decreasing the reliance on its affected sections. One way to do this is to reduce the power flow through lines vulnerable to severe weather. If a line is disconnected, its initial power flow is distributed through the neighbor lines, which may cause congestion in the grid. FACTS devices can be used to control the power flow of lines that have a higher chance of power outages. Most previous works do not consider weather events in power flow control. In this work, a linearized optimal power flow (OPF)–based algorithm is developed to minimize the real power flow of vulnerable lines considering the thermal limits of lines to prevent infeasible solutions; the simulation is fast, making it suitable for large-scale systems. The proposed optimization problem is presented as a mixed-integer linear program (MILP), making it capable of using short-term load forecasting due to its high solution speed. The proposed optimization problem considers multiple lines with different outage probabilities and the uncertainties of the weather forecast. Moreover, it estimates the power reduction in vulnerable lines due to changes in the series FACTS devices. The performance of the proposed optimization problem is tested on IEEE 14-, 30-, and 118-bus systems for several scenarios. The results are validated with the AC power flow results from MATPOWER.

Keywords: FACTS devices; MILP; optimal power flow; power flow; resiliency; severe weather; uncertainty modeling

Citation: Beikbabaei, M.; Mehrizi-Sani, A. Series FACTS Devices for Increasing Resiliency in Severe Weather Conditions. *Energies* **2023**, *16*, 5866. https://doi.org/10.3390/en16165866

Academic Editors: Akhtar Kalam and David Macii

Received: 26 May 2023
Revised: 4 August 2023
Accepted: 5 August 2023
Published: 8 August 2023

1. Introduction

Severe weather conditions are low-probability, high-impact events that affect grid operations. About 50% of power outage events in the United States are associated with severe weather [1]. Severe weather conditions are happening more frequently, possibly due to global warming [2]. They can decrease grid resiliency by causing transmission line outages, power outages, and blackouts. Moreover, the increase in electricity demand during the past decades has congested the overhead lines, decreased the stability of the grid, and decreased the security of the power grid.

Many studies have been conducted on weather-related outage probability using different methods. Reference [3] uses numerical weather prediction integrated with machine learning algorithms to increase the ability to forecast severe weather conditions to increase the resiliency of the transmission system on the Greek electricity grid. Reference [4] uses machine learning-based methods to predict power outages for up to five days; however, the prediction uncertainly decreases as it predicts the outage probability of the next three days. Reference [5] improves outage prediction due to extreme weather, testing several methods. Reference [6] utilizes spatial and temporal variation to estimate transmission line outages due to severe weather. Reference [7] uses a Bayesian-based method to predict power outages using radar measurements data. Reference [8] uses a comparative analysis of numeric weather prediction of different layers to predict thunderstorm-related power

outages. In this work, the line outage probability is considered as input to the algorithm; however, the uncertainty of the weather prediction is considered as well.

Research on reducing the impact of severe weather effects on the grid, increasing grid stability, and increasing grid security is extensive. Reference [9] proposes a simulation-based optimization to mitigate cascading outages in severe weather using day-ahead weather forecasts applying a near-optimal hardening decision. Reference [10] proposes an optimization problem for power outage scheduling considering covariance in power systems and maintenance outage scheduling. However, it takes about 84 h for one of the cases implemented on the IEEE 118-bus with 40 scenarios. Reference [11] develops a bi-level optimization to reconfigure the distributed grid to improve the resiliency to extreme weather, where short-term weather forecasting cannot be used.

If a transmission line is disconnected, its power flow drops to zero and is distributed through the neighbor lines, which can cause congestion. The impacts of transmission line outages can be reduced by decreasing the power flow of lines that are vulnerable to severe weather. Power routing can modify the power through lines and can be used to decrease the criticality of vulnerable lines to severe weather. On-load tap changer and phase shifting transformers are among the first technologies used for power routing. They are used in static control since they are mechanical, slow, and enable discrete control with a large range. Reference [12] uses a phase-shifting transformer for controlling the power flow. With significant improvements in power electronics, more power electronic-based devices, such as flexible AC transmission system (FACTS) devices and HVDC, are being used for power routing. FACTS devices can be used for increasing the system loadability, increasing system stability, and reducing the transmission loss [13,14]. The series FACTS device can change the impedance of the line to which it is connected and is modeled as a modification to the line impedance in the steady state. The optimization problem deals with steady-state performance, and, as such, it is agnostic to the particular type of series FACTS device that is used: SSSC, physical capacitor, or devices such as distributed FACTS.

Reference [15] investigates the power routing capability of line current commutated HVDC to absorb the fluctuations of the wind power connected through an HVDC line system to an AC grid. Reference [16] proposes an extension of the security constrained OPF, to enable inclusion of the real-time dispatchable resources. However, references [15,16] do not consider the impact of severe weather. Reference [17] uses a corrective topology control method to enhance grid security. However, it does not consider the impact of severe weather, cannot respond before a contingency, and cannot be used for real-time applications. Reference [18] uses transmission network topology control to determine the optimal topology considering system reliability concerns. Reference [19] proposes a selective power routing method that provides primary frequency support to decrease the disturbances. References [18,19] do not consider severe weather impact. Reference [20] uses matrix perturbation for tuning series FACTS devices to decrease the real power flow through lines vulnerable to severe weather. However, it does not consider the thermal limits of lines, which may result in infeasible solutions. Moreover, it does not consider multiple affected lines with different outage probabilities and does not estimate the real power reduction in lines vulnerable to series FACTS device tuning.

An OPF-based algorithm can be used to solve the power routing problem. Reference [21] proposes a generic power flow routing algorithm to increase the loadability of the system using an OPF-based algorithm. Since the power flow equations are nonconvex, it uses semidefinite programming relaxation to convex the problem and find the near-optimal or optimal solutions. Reference [22] proposes a generic steady-state model for energy routers using an OPF-based algorithm. It shows that the power system operation can be optimized by controlling the power injection and voltage of the energy routers.

This paper proposes a linearized OPF-based algorithm for minimizing the real power flow through lines vulnerable to severe weather by tuning series FACTS devices. The algorithm is developed based on DC power flow. AC power flow considers active and reactive power, which makes it a nonlinear problem where the Newton–Raphson algorithm

can be used to solve it. The AC power flow solving time increases with the system size as well [23]. DC power flow is the linearized version of AC load flow where the reactive power is neglected. DC power flow solutions are non-iterative, simple, can be optimized efficiently, and can approximate real power flows reasonably accurately [24]. Reference [25] develops a novel DC power flow method with reactive power consideration. Reference [26] extends the DC power flow and considers the voltage magnitude to increase DC power flow accuracy. Reference [20] develops a formulation based on the Sherman–Morrison formula for power routing using series FACTS devices with DC load flow. The formulation is validated on various scenarios on both IEEE 14- and 118-bus systems. The line outage probability is based on available weather forecast data. Unlike previous work, it considers the thermal limits of lines, estimates the real power flow reduction in affected lines, and can consider multiple lines with different outage probabilities. The OPF is solved using a mixed-integer linear program (MILP), which results in the optimal global solutions. Solving the nonlinear problem does not guarantee the optimal global solution and may get stuck in the local optimum instead. Moreover, it takes longer to solve the nonlinear algorithm compared to the linearized problem.

The main contribution of this paper is developing an OPF-based algorithm using series FACTS devices to increase grid resiliency with the following characteristics:

- The linearized algorithm guarantees finding the optimal solution and estimates the real power flow reduction in the affected lines.
- The optimization problem can consider lines with different outage probabilities simultaneously.
- It considers the thermal limits of lines.
- Since the algorithm is linear, it is solved quickly, making it suitable for implementation in large transmission grids.
- The simulation is fast, enabling the use of short-term weather forecast input to increase accuracy.
- The uncertainties in the outage probability are modeled using scenario-based methods [27,28].

2. Problem Formulation

The problem formulation is considered in the following discussion. First, series FACTS devices are added to the DC power flow formulation, then the severe weather effects are added to the OPF-based formulation. Finally, the weather forecast uncertainties are discussed.

2.1. FACTS Devices in the DC Power Flow

In DC power flow, voltages are fixed at 1 pu for all buses, and the inclusion of reactive powers and branch resistances is neglected. DC power flow calculates only the real power injected into buses and the real power going through the lines. DC power flow equations of lines and buses are shown in the following:

$$\begin{aligned} 0 &= -P_{\text{branch}} + D\,A\,\theta \\ 0 &= -P_{\text{bus}} + B\,\theta, \end{aligned} \tag{1}$$

where B is the susceptance matrix, D is the diagonal matrix of the lines susceptance, A is the incidence matrix, θ is the bus angle matrix, P_{bus} is the real power injected to the buses, and P_{branch} is the real power going through the lines. A series FACTS device changes the line impedance, which, in turn, changes the B and D matrices, but not P_{bus}. However, θ and P_{branch} do change. The updated values of θ, D, B, and P_{branch} are shown in the following:

$$\begin{aligned} \theta &= \theta_{\text{prev}} + \Delta\theta \\ D &= D_{\text{prev}} + \Delta D \\ B &= B_{\text{prev}} + \Delta B \\ P_{\text{branch}} &= P_{\text{branch-prev}} + \Delta P_{\text{branch}}, \end{aligned} \tag{2}$$

where θ_{prev}, D_{prev}, B_{prev}, and $P_{\text{branch-prev}}$ are the initial values before updating the series FACTS device, and $\Delta\theta$, ΔD, ΔB, and ΔP_{branch} are the differences between the updated and the initial values. Substituting (2) in (1) results in (3):

$$\begin{aligned} 0 &= -\Delta P_{\text{branch}} + D_{\text{prev}} A \Delta\theta + \Delta D A \theta_{\text{prev}} + \Delta D A \Delta\theta \\ 0 &= B_{\text{prev}} \Delta\theta + \Delta B \theta_{\text{prev}} + \Delta B \Delta\theta. \end{aligned} \tag{3}$$

Equation (3) is nonlinear due to the terms $\Delta D A \Delta\theta$ and $\Delta B \Delta\theta$. By tuning the series FACTS devices, the impedance of lines with installed series FACTS devices changes, but not the impedance of other lines. For ΔD, only the diagonal elements of lines with series FACTS devices change around 20% since the series FACTS devices can only change around 20% of the line impedance. For ΔB, only elements of buses that are connected to the series FACTS devices change. $\Delta\theta$ changes due to the small changes in ΔD and the ΔB matrices. The nonlinear terms are relatively small compared to the other terms and can be neglected. Thus, (3) can be written as the following:

$$\begin{aligned} 0 &= -\Delta P_{\text{branch}} + D_{\text{prev}}\, A\, \Delta\theta + \Delta D\, A\, \theta_{\text{prev}} \\ 0 &= B_{\text{prev}}\, \Delta\theta + \Delta B\, \theta_{\text{prev}}, \end{aligned} \tag{4}$$

where (4) shows the linearized power flow equation integrated with series FACTS devices. ΔB and ΔD can be written as a multiplication of a scalar, representing the change in the line susceptance with a series FACTS device, and a fixed matrix containing one, minus one, and zero elements, which is shown in the following:

$$\begin{aligned} \Delta B &= \Delta b\, \Delta B_{\text{matrix}} \\ \Delta D &= \Delta b\, \Delta D_{\text{matrix}}, \end{aligned} \tag{5}$$

where Δb represents the susceptance changes of lines with the series FACTS device, and ΔB_{matrix} and ΔD_{matrix} are fixed matrices. For example, the nonzero elements of the fixed matrices are shown in (6) where the line k has a series FACTS device connected to buses i and j.

$$\begin{aligned} \Delta B_{\text{matrix}}(i,i) &= \Delta B_{\text{matrix}}(j,j) = 1 \\ \Delta B_{\text{matrix}}(i,j) &= \Delta B_{\text{matrix}}(j,i) = -1 \\ \Delta D_{\text{matrix}}(k,k) &= 1. \end{aligned} \tag{6}$$

Substituting (5) in (4) results in (7):

$$\begin{aligned} 0 &= -\Delta P_{\text{branch}} + D_{\text{prev}}\, A\, \Delta\theta + \Delta b\, \Delta D_{\text{matrix}}\, A\, \theta_{\text{prev}} \\ 0 &= B_{\text{prev}}\, \Delta\theta + \Delta b\, \Delta B_{\text{matrix}}\, \theta_{\text{prev}}. \end{aligned} \tag{7}$$

2.2. Inclusion of Severe Weather

Equation (8) is the matrix representation of (7), where m is the branch number, and n is the bus number.

$$\begin{bmatrix} -\mathbf{I}(m,m) & D_{\text{prev}} A & \Delta D_{\text{matrix}} A \theta_{\text{prev}} \\ \mathbf{O}(n-1,m) & B_{\text{prev}} & \Delta B_{\text{matrix}} \theta_{\text{prev}} \end{bmatrix} \begin{bmatrix} \Delta P_{\text{branch}} \\ \Delta\theta \\ \Delta b \end{bmatrix} = \begin{bmatrix} 0 \\ \vdots \\ 0 \end{bmatrix}. \tag{8}$$

The objective function is shown in the following:

$$\min \sum_{i=1}^{n} E_{\mathrm{i}}\, P_{\mathrm{branch},i\mathrm{th}}, \tag{9}$$

where E_{i} is the probability of line i outage, which is between zero and one, and $P_{\mathrm{branch},i\mathrm{th}}$ is the real power that goes through line i. $\Delta P_{\mathrm{branch}}$, $\Delta\theta$, and Δb are the optimization variables.

To decrease the criticality of the target line, the absolute value of the real power going through it should decrease. Algorithm 1 shows the algorithm which is used to determine the sign of E_{i} in a way that (9) decreases the absolute value of the real power for positive and negative values of the real power flow.

Algorithm 1 Determining sign of E_i.

```
for i = 1 to m do
    if (P_branch,ith ≥ 0) then
        E_i = E_i
    else
        E_i = −E_i
    end if
end for
```

The minimum power which can go through the line is zero. An inequality constraint is added to prevent the direction change of target line power flow, as shown in the following:

$$\mathrm{Sign}_{\text{target line}}\, \Delta P_{\text{target lines}} \leq |P_{\text{target lines}}|, \tag{10}$$

where $\mathrm{Sign}_{\text{target line}}$ is determined considering the sign of the real power going through the lines, as shown in Algorithm 2. The thermal limits of the lines are added using (11).

$$-P_{\text{thermal}} \leq \Delta P_{\text{branch}} + P_{\text{branch prev}} \leq P_{\text{thermal}}. \tag{11}$$

Algorithm 2 Preventing target line power direction change.

```
for i = 1 to num-target-line do
    if (P_target line ≥ 0) then
        Sign_target line = −1
    else
        Sign_target line = 1
    end if
end for
```

2.3. Inclusion of Weather Forecast Uncertainties

Reference [28] reviews different methods to model uncertainty in power systems. A scenario-based method is an analytical model for studying the uncertain input using the probability density function (PDF). The scenario-based method is simple and efficient, but it yields an approximation of the expected value function. In the scenario-based method, the continuous PDF function, $f(\mathrm{x})$, is split into N regions, where the corresponding probabilities are $P_1, P_2, ..., P_N$, and the expected value is calculated as follows [27,28]:

$$E(\mathrm{y}) = \sum_{k=1}^{N} P_{\mathrm{k}}\, f(\mathrm{x}), \tag{12}$$

where the algorithm runs for N different probabilities, and (12) can be used to consider uncertainties to tune the series FACTS device. By increasing N, the accuracy of the proposed optimization problem will increase; however, the simulation time increases.

3. Proposed Methodology

The desirable susceptance of series FACTS devices is calculated using the OPF-based algorithm using (8)–(11), which are based on the DC power flow formulations. The flowchart of the proposed optimization problem is shown in Figure 1. The susceptance matrix, diagonal matrix of line susceptance, thermal limits of lines, line *A* outage probability, line *B* outage probability, lines real power, buses real power injection, and the buses voltage angle are the input of the proposed algorithm. The line *A* updated real power, the line *B* updated real power, and the series FACTS device susceptance are the algorithm outputs. Equations (10) and (11) are the algorithm constraints.

The calculated change in the real power of the lines due to topology changes using DC power flow provides results that are equivalent to the changes calculated by the AC power flow. However, calculating the real power of the lines using DC power flow produces some errors compared to the AC power flow. The proposed optimization problem is tested on different grids for different outage probabilities, and the results are compared with the AC power flow results. In the case of multiple series FACTS devices, a scalar optimization variable must be considered for each of the series FACTS devices.

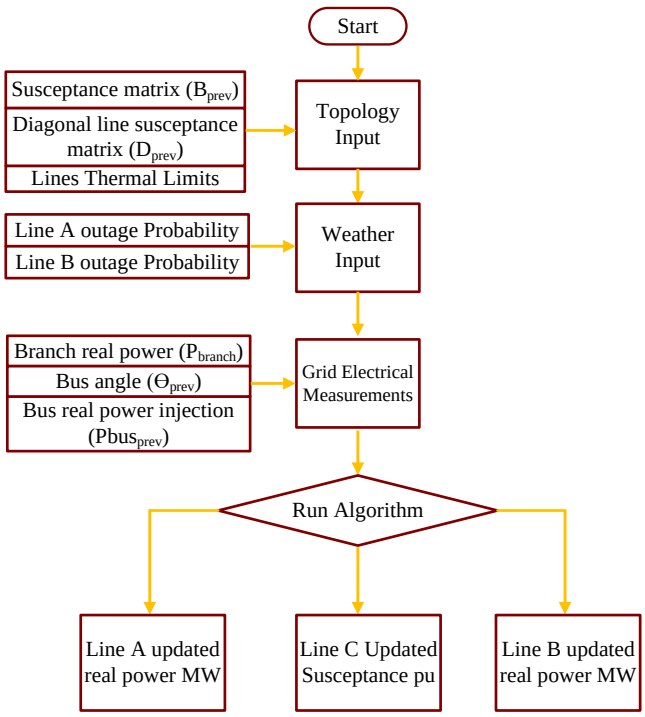

Figure 1. Flowchart of the proposed algorithm.

4. Simulation Results

The various simulation studies were performed on IEEE 14-, 30-, and 118-bus systems. Line *A* and *B* were selected as target lines vulnerable to power outages. A series FACTS device was installed on line *C*, and four different cases were simulated for each IEEE system. The calculations were performed using a Core i7 computer with 16 GB RAM. It took about 11 ms for the proposed optimization problem to calculate the optimal value for the series FACTS devices for the IEEE 118-bus system, which makes it applicable to electrical grids with thousands of buses. Case *D* shows the importance of considering the thermal limits of lines and how [20] can lead to infeasible solutions. The AC power flow was calculated using the MATPOWER toolbox to validate the proposed optimization problem results [29]. A comparison of the simulation results for various scenarios with AC power flow from MATPOWER is shown in Table 1. In addition, one scenario considering uncertainties on the IEEE 14-bus system was simulated.

Table 1. Performance comparison of the proposed optimization problem for different IEEE systems.

System	Probability Outage Line A	Probability Outage Line B	Calculated Susceptance Change in (pu) Using Proposed Method	Calculated Susceptance Change in (pu) Using AC LDF	Line A Initial Real Power (MW) Using AC LDF	Line A Updated Real Power (MW) Using AC LDF	Line B Initial Real Power (MW) Using AC LDF	Line B Updated Real Power (MW) Using AC LDF	Time (ms)
14-bus	0	1	1.1343	1.1343	28.0743	28.2238	44.0872	43.8493	4
	1	0	−1.1343	−1.1343	28.0743	27.8862	44.0872	44.3882	4
	0.66	0.33	−1.1343	−1.1343	28.0743	27.8862	44.0872	44.3882	4
	0.33	0.66	1.1343	1.1343	28.0743	28.2238	44.0872	43.8493	4
30-bus	0	1	5	5	−1.6716	−1.6649	24.8223	24.8219	7
	1	0	5	5	−1.6716	−1.6649	24.8223	24.8219	7
	0.7	0.3	5	5	−1.6716	−1.6649	24.8223	24.8219	7
	0.3	0.7	5	5	−1.6716	−1.6649	24.8223	24.8219	7
118-bus line C thermal limit is 80 MW	0	1	1.8518	1.8518	16.4788	14.7552	64.2297	62.6855	11
	1	0	1.8519	1.8518	16.4788	14.7552	64.2297	62.6855	11
	0.6	0.4	1.8519	1.8518	16.4788	14.7552	64.2297	62.6855	11
	0.4	0.6	1.8518	1.8518	16.4788	14.7552	64.2297	62.6855	11
118-bus line C thermal limit is 70 MW	0	1	0.51	0.51	16.4788	15.968	64.2297	63.772	11
	1	0	0.51	0.51	16.4788	15.968	64.2297	63.772	11
	0.6	0.4	0.51	0.51	16.4788	15.968	64.2297	63.772	11
	0.4	0.6	0.51	0.51	16.4788	15.968	64.2297	63.772	11

4.1. IEEE 14-Bus

Line A is between buses 7 and 9, line B is between buses 5 and 6, and line C is between buses 2 and 4. The same lines as [20] are selected for comparing the results. The design line and target lines for the IEEE 14-bus system are shown in Figure 2. In all four cases, the algorithm reduces the criticality of the vulnerable lines considering different outage probabilities.

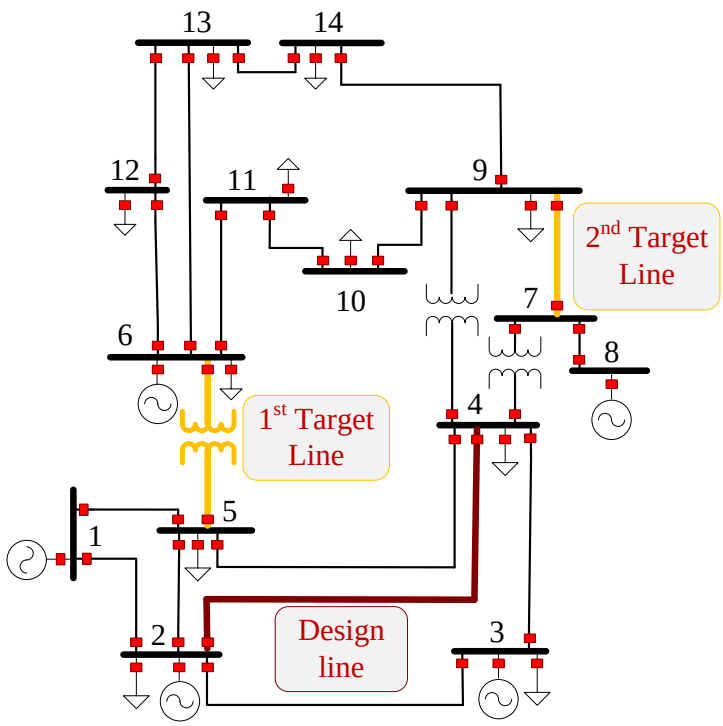

Figure 2. IEEE 14-bus system target and design lines.

4.1.1. Case 1: Outage Probability of Line A = 100%

The probability of line A outage is 100%. The line A AC power flow result is shown in Figure 3a. By decreasing the line C susceptance by 1.1343 pu, 20%, the line B real power decreases by 0.1881 MW, 0.67%. The results for this scenario are the same as reported in reference [20].

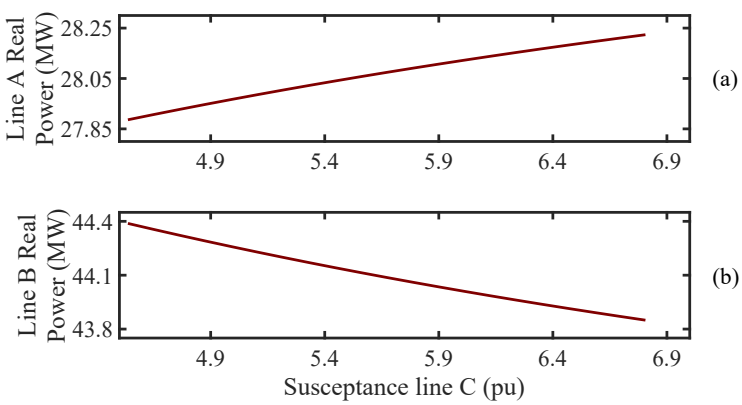

Figure 3. The real power change in target lines in the IEEE 14-bus system by changing the susceptance of line C with 0.01 pu steps, and, in each step, the real power is calculated using MATPOWER AC power flow. (**a**) For line A, (**b**) for line B.

4.1.2. Case 2: Outage Probability of Line *B* = 100%

The probability of line *B* outage is 100%. The line *B* AC power flow result is shown in Figure 3b. By increasing the line *C* susceptance by 1.1343 pu, 20%, the line *B* real power decreases by 0.2379 MW, 0.54%. The results for this scenario are the same as reported in reference [20].

4.1.3. Case 3: Outage Probability of Line *A* = 66% and *B* = 33%

The probability of line *B* outage is 33%, and the probability of line *A* outage is 66%. By decreasing the line *C* susceptance by 1.1343 pu, 20%, the line *A* real power decreases by 0.1881 MW, 0.67%, and the line *B* real power increases by 0.3010 MW, 0.68%. The weighted real power is decreased by 0.0903 MW.

4.1.4. Case 4: Outage Probability of Line *A* = 33% and *B* = 66%

The probability of line *B* outage is 66%, and the probability of line *A* outage is 33%. By increasing the line *C* susceptance by 1.1343 pu, 20%, the line *B* real power decreases by 0.2379 MW, 0.54%, and the line *A* real power increases by 0.1495 MW, 0.53%. The weighted real power is decreased by 0.2202 MW.

4.2. IEEE 30-Bus

Line *A* is between buses 4 and 12, line *B* is between buses 6 and 8, and line *C* is between buses 3 and 4. Line *A* is selected since the real power going through it is negative. The design line and target lines are shown in Figure 4. Line *A* is selected since it has negative real power. The real power reduction for all scenarios is small. Moreover, the algorithm estimates the reduction correctly, indicating that tuning the series FACT device for lines *A* and *B* does not significantly decrease their criticality.

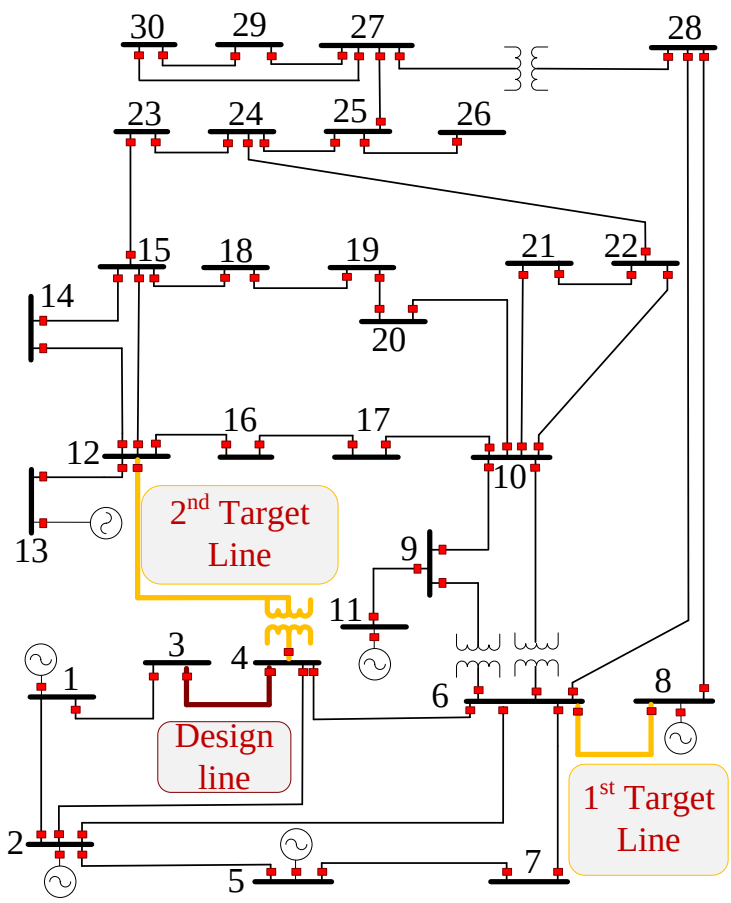

Figure 4. IEEE 30-bus system target and design lines.

4.2.1. Case 1: Outage Probability of Line A = 100%

The probability of line A outage is 100%. The line A AC power flow result is shown in Figure 5a. By increasing the line C susceptance by 5 pu, 20%, the line A real power decreases by 0.0067 MW, 0.4%.

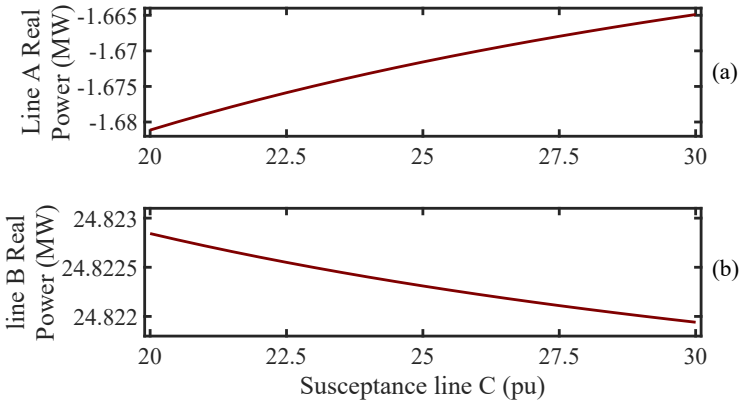

Figure 5. The real power change in target lines in the IEEE 30-bus system by changing the susceptance of line C with 0.01 pu steps, and, in each step, the real power is calculated using MATPOWER AC power flow. (**a**) For line A, (**b**) for line B.

4.2.2. Case 2: Outage Probability of Line B = 100%

The probability of line B outage is 100%. The line B AC power flow result is shown in Figure 5b. By increasing the line C susceptance by 5 pu, 20%, the line B real power decreases by 0.0004 MW, 0.002%.

4.2.3. Case 3: Outage Probability of Line A = 70% and B = 30%

The probability of line B outage is 30%, and the probability of line A outage is 70%. By increasing the line C susceptance by 5 pu, 20%, the line A real power decreases by 0.0067 MW, 0.4%, and the line B real power decreases by 0.0004 MW, 0.002%.

4.2.4. Case 4: Outage Probability of Line A = 30% and B = 70%

The probability of line B outage is 70%, and the probability of line A outage is 30%. By increasing the line C susceptance by 5 pu, 20%, the line A real power decreases by 0.0067 MW, 0.4%, and the line B real power decreases by 0.0004 MW, 0.002%.

4.3. IEEE 118-Bus

Line A is between buses 7 and 12, line B is between buses 4 and 11, and line C is between buses 3 and 5. Lines A and B are selected in a way that the real power going through them changes significantly by changing the line C susceptances. The line A real power decreases by 10.46% by increasing the line C susceptance. The thermal limits of the line C is 80 MW in this case.

4.3.1. Case 1: Outage Probability of Line A = 100%

The probability of line A outage is 100%. The line A and line C AC power flow results are shown in Figure 6a,c. By increasing the line C susceptance by 1.8519 pu, 20%, the line A real power decreases by 1.7236 MW, 10.46%. The line C real power becomes −75 MW and is lower than its thermal limits.

4.3.2. Case 2: Outage Probability of Line B = 100%

The probability of line B outage is 100%. The line B and line C AC power flow results are shown in Figure 6b,c. By increasing the line C susceptance by 1.8519 pu, 20%, the line B real power decreases by 1.5442 MW, 2.4%. The line C real power becomes −75 MW and is lower than its thermal limits.

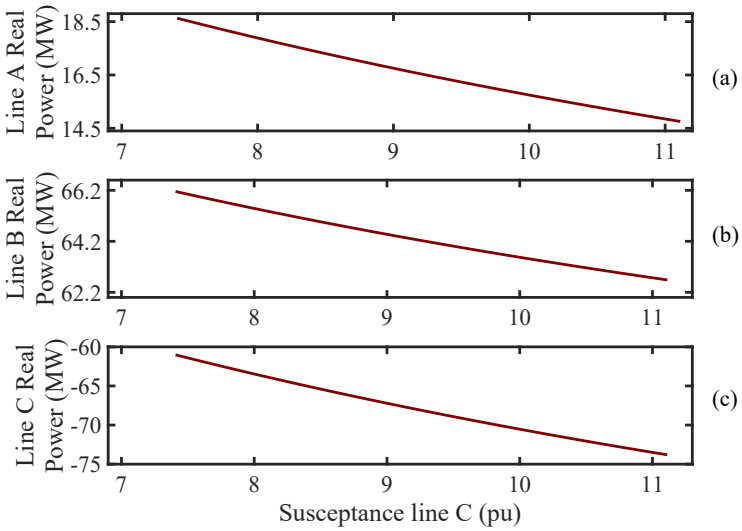

Figure 6. The real power change in the target and design lines in the IEEE 118-bus system by changing the susceptance of line *C* with 0.01 pu steps, and, in each step, the real power is calculated using MATPOWER AC power flow. (**a**) For line *A*, (**b**) for line *B*, (**c**) for line *C*.

4.3.3. Case 3: Outage Probability of Line *A* = 60% and *B* = 40%

The probability of line *B* outage is 40%, and the probability of line *A* outage is 60%. By increasing the line *C* susceptance by 1.8519 pu, 20%, the line *A* real power decreases by 1.7236 MW, 10.46%, and the line *B* real power decreases by 1.5442 MW, 2.4%.

4.3.4. Case 4: Outage Probability of Line *A* = 60% and *B* = 40%

The probability of line *B* outage is 60%, and the probability of line *A* outage is 40%. By increasing the line *C* susceptance by 1.8519 pu, 20%, the line *A* real power decreases by 1.7236 MW, 10.46%, and the line *B* real power decreases by 1.5442 MW, 2.4%.

4.4. IEEE 118-Bus with thermal Limits

Line *A*, *B*, and *C* are the same as section *C*. The thermal limits of line *C* is 70 MW, which is a different result compared to section *C*. The line *C* thermal limit is 70 MW in this case.

4.4.1. Case 1: Outage Probability of Line *A* = 100%

The probability of line *A* outage is 100%. The line *A* and line *C* AC power flow results are shown in Figure 6a,c. By increasing the line *C* susceptance by 0.51 pu, 5.5%, the line *A* real power decreases by 0.5108 MW, 3.1%, and the line *C* reaches its thermal limits.

4.4.2. Case 2: Outage Probability of Line *B* = 100%

The probability of line *B* outage is 100%. The line *B* and line *C* AC power flow results are shown in Figure 6b,c. By increasing the line *C* susceptance by 0.51 pu, 5.5%, the line *B* real power decreases by 0.4577 MW, 0.71%, and the line *C* reaches its thermal limits.

4.4.3. Case 3: Outage Probability of Line *A* = 60% and *B* = 40%

The probability of line *B* outage is 40%, and the probability of line *A* outage is 60%. By increasing the line *C* susceptance by 0.51 pu, 5.5%, the line *A* real power decreases by 0.5108 MW, 3.1%, and the line *B* real power decreases by 0.4577 MW, 0.71%.

4.4.4. Case 4: Outage Probability of Line *A* = 40% and *B* = 60%

The probability of line *B* outage is 60%, and the probability of line *A* outage is 40%. By increasing the line *C* susceptance by 0.51 pu, 5.5%, the line *A* real power decreases by 0.5108 MW, 3.1%, and the line *B* real power decreases by 0.4577 MW, 0.71%.

4.5. IEEE 14-Bus with Uncertainty in Outage Probability

The probability of the outage of line B is 33%, and the probability of outage of line A is 66%; however, the outage PDF function has a normal Gaussian distribution with a standard deviation of 0.15 and mean of 0.66, as shown in Figure 7. Using (12) and Table 1, the susceptance of the series FACTS device is calculated, as shown in the following:

$$E(\mathrm{S}) = \sum_{k=1}^{4} P_{\mathrm{k}}\, S(\mathrm{k}) = P_1\, S_1 + P_2\, S_2 + P_3\, S_3 + P_4\, S_4 = -0.5150. \tag{13}$$

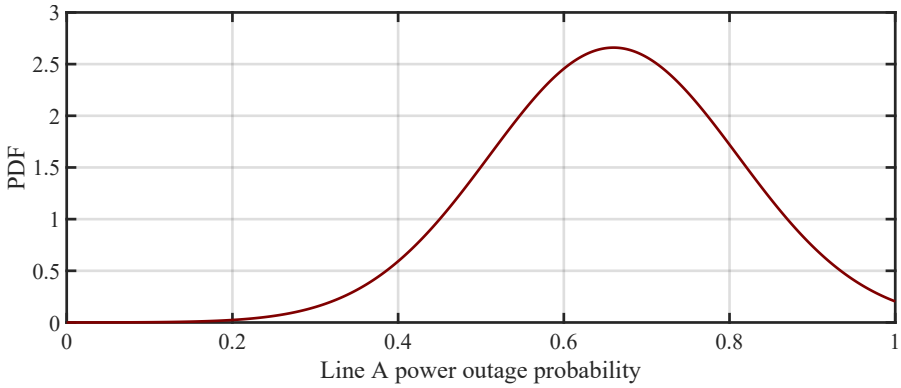

Figure 7. The PDF curve of the outage of line A for IEEE 14-bus system.

Without considering the uncertainties in the outage probabilities, the series FACTS device susceptance is −1.1343 pu. Considering the aforementioned uncertainties, it is −0.515 pu.

4.6. Comparison Between Case Studies

The proposed optimization problem correctly finds the designed line susceptance values in all 16 scenarios, which minimize the target line power flow, as shown in Table 1. Moreover, the proposed optimization problem can consider the thermal limits of lines to prevent infeasible solutions, which is shown in the IEEE 118-bus with thermal limits, the last four cases. The proposed optimization problem estimates the power loss, which helps to estimate the power flow reduction for the target lines. In some cases, the target line power flow is reduced significantly, such as when the outage probability in Line A is 1 in the IEEE 118-bus system without thermal limits of lines, where the real line power is reduced by 10.46%. However, in some scenarios, the target line power is reduced slightly, such as in the first scenario of the IEEE 30-bus system, where the target line real power is only reduced by 0.002%. Finally, the uncertainty in the outage probability is simulated on the IEEE 14-bus system.

5. Conclusions

Around half of power outages in the United States are associated with severe weather conditions. The impact of these severe weather conditions can be reduced by reducing the real power through lines vulnerable to severe weather. Series FACTS devices can be used for this purpose. This paper proposes a linearized optimal power flow (OPF)–based algorithm to minimize the real power flow of vulnerable lines to severe weather. It can consider multiple lines with different outage probabilities based on available weather forecast data. Moreover, the OPF-based formulation is solved using a mixed-integer linear program (MILP). The proposed optimization problem is studied on IEEE 14-, 30-, and 118-bus systems, and four different outage probabilities of two lines vulnerable to power outage are considered. Moreover, a 70 MW thermal limit of line C is considered for the IEEE 118-bus system, and the results indicate that not considering the thermal limits of lines will lead to infeasible results. All the simulation results were verified using AC power

flow calculated using MATPOWER. It takes about 11 ms for the proposed optimization problem to calculate the optimal value for impedance of the series FACTS devices for the IEEE 118-bus system, which makes it applicable to large grids with thousands of buses and suitable for using short-term weather forecasts. The uncertainty in the weather forecast is simulated on the IEEE 14-bus system using a scenario-based method.

Author Contributions: Writing—original draft: M.B.; writing—review and editing: A.M.-S. All authors have read and agreed to the published version of the manuscript.

Funding: This work is supported in part by National Science Foundation (NSF) under award ECCS-1953213, in part by the State of Virginia's Commonwealth Cyber Initiative (www.cyberinitiative.org), and in part by the U.S. Department of Energy's Office of Energy Efficiency and Renewable Energy (EERE) under the Solar Energy Technologies Office Award Number 38637 (UNIFI Consortium). The views expressed herein do not necessarily represent the views of the U.S. Department of Energy or the United States Government.

Institutional Review Board Statement: Not applicable.

Informed Consent Statement: Not applicable.

Data Availability Statement: Not applicable.

Conflicts of Interest: The authors declare no conflict of interest.

References

1. Taimoor, N.; Khosa, I.; Jawad, M.; Akhtar, J.; Ghous, I.; Qureshi, M.B.; Ansari, A.R.; Nawaz, R. Power Outage Estimation: The Study of Revenue-Led Top Affected States of United States. *IEEE Access* **2020**, *8*, 223271–223286. [CrossRef]
2. Younesi, A.; Shayeghi, H.; Wang, Z.; Siano, P.; Mehrizi-Sani, A.; Safari, A. Trends in modern power systems resilience: State-of-the-art review. *Renew. Sustain. Energy Rev.* **2022**, *162*, 112397. [CrossRef]
3. Zafeiropoulou, M.; Mentis, I.; Sijakovic, N.; Terzic, A.; Fotis, G.; Maris, T.I.; Vita, V.; Zoulias, E.; Ristic, V.; Ekonomou, L. Forecasting Transmission and Distribution System Flexibility Needs for Severe Weather Condition Resilience and Outage Management. *Appl. Sci.* **2022**, *12*, 7334. [CrossRef]
4. Yang, F.; Cerrai, D.; Anagnostou, E.N. The Effect of Lead-Time Weather Forecast Uncertainty on Outage Prediction Modeling. *Forecasting* **2021**, *3*, 501–516. [CrossRef]
5. Watson, P.L.; Spaulding, A.; Koukoula, M.; Anagnostou, E. Improved quantitative prediction of power outages caused by extreme weather events. *Weather. Clim. Extrem.* **2022**, *37*, 100487. [CrossRef]
6. Yang, S.; Zhou, W.; Zhu, S.; Wang, L.; Ye, L.; Xia, X.; Li, H. Failure probability estimation of overhead transmission lines considering the spatial and temporal variation in severe weather. *J. Mod. Power Syst. Clean Energy* **2019**, *7*, 131–138. [CrossRef]
7. Yue, M.; Toto, T.; Jensen, M.P.; Giangrande, S.E.; Lofaro, R. A Bayesian Approach-Based Outage Prediction in Electric Utility Systems Using Radar Measurement Data. *IEEE Trans. Smart Grid* **2018**, *9*, 6149–6159. [CrossRef]
8. Watson, P.L.; Koukoula, M.; Anagnostou, E. Influence of the Characteristics of Weather Information in a Thunderstorm-Related Power Outage Prediction System. *Forecasting* **2021**, *3*, 541–560. [CrossRef]
9. Xu, J.; Yao, R.; Qiu, F. Mitigating Cascading Outages in Severe Weather Using Simulation-Based Optimization. *IEEE Trans. Power Syst.* **2021**, *36*, 204–213. [CrossRef]
10. Wang, Y.; Li, Z.; Shahidehpour, M.; Wu, L.; Guo, C.X.; Zhu, B. Stochastic Co-Optimization of Midterm and Short-Term Maintenance Outage Scheduling Considering Covariates in Power Systems. *IEEE Trans. Power Syst.* **2016**, *31*, 4795–4805. [CrossRef]
11. Khomami, M.S.; Jalilpoor, K.; Kenari, M.T.; Sepasian, M.S. Bi-level network reconfiguration model to improve the resilience of distribution systems against extreme weather events. *IET Gener. Transm. Distrib.* **2019**, *13*, 3302–3310. [CrossRef]
12. Iravani, M.; Dandeno, P.; Nguyen, K.; Zhu, D.; Maratukulam, D. Applications of static phase shifters in power systems. *IEEE Trans. Power Deliv.* **1994**, *9*, 1600–1608. [CrossRef]
13. Abido, M. Power system stability enhancement using FACTS controllers: A review. *Arab. J. Sci. Eng.* **2009**, *34*, 153–172.
14. Gandoman, F.H.; Ahmadi, A.; Sharaf, A.M.; Siano, P.; Pou, J.; Hredzak, B.; Agelidis, V.G. Review of FACTS technologies and applications for power quality in smart grids with renewable energy systems. *Renew. Sustain. Energy Rev.* **2018**, *82*, 502–514. [CrossRef]
15. Yin, H.; Fan, L.; Miao, Z. Fast power routing through HVDC. *IEEE Trans. Power Deliv.* **2012**, *27*, 1432–1441. [CrossRef]
16. Thomas, J.J.; Grijalva, S. Flexible security-constrained optimal power flow. *IEEE Trans. Power Syst.* **2015**, *30*, 1195–1202. [CrossRef]
17. Korad, A.S.; Hedman, K.W. Robust Corrective Topology Control for System Reliability. *IEEE Trans. Power Syst.* **2013**, *28*, 4042–4051. [CrossRef]
18. Li, X.; S Korad, A.; Balasubramanian, P. Sensitivity factors based transmission network topology control for violation relief. *IET Gener. Transm. Distrib.* **2020**, *14*, 3539–3547. [CrossRef]

19. Vennelaganti, S.G.; Chaudhuri, N.R. Selective power routing in MTDC grids for inertial and primary frequency support. *IEEE Trans. Power Syst.* **2018**, *33*, 7020–7030. [CrossRef]
20. Mehrizi-Sani, A.; Koorehdavoudi, K.; Roy, S. Power Routing by Impedance Modulation. In Proceedings of the 11th Bulk Power Systems Dynamics and Control Symposium, Banff, AB, Canada, 25–30 July 2022.
21. Lin, J.; Li, V.O.K.; Leung, K.C.; Lam, A.Y.S. Optimal Power Flow With Power Flow Routers. *IEEE Trans. Power Syst.* **2017**, *32*, 531–543. [CrossRef]
22. Miao, J.; Zhang, N.; Kang, C.; Wang, J.; Wang, Y.; Xia, Q. Steady-State Power Flow Model of Energy Router Embedded AC Network and Its Application in Optimizing Power System Operation. *IEEE Trans. Smart Grid* **2018**, *9*, 4828–4837. [CrossRef]
23. Van Hertem, D.; Verboomen, J.; Purchala, K.; Belmans, R.; Kling, W. Usefulness of DC power flow for active power flow analysis with flow controlling devices. In Proceedings of the 8th IEE International Conference on AC and DC Power Transmission, London, UK, 28–31 March 2006; pp. 58–62. [CrossRef]
24. Stott, B.; Jardim, J.; Alsac, O. DC Power Flow Revisited. *IEEE Trans. Power Syst.* **2009**, *24*, 1290–1300. [CrossRef]
25. Fatemi, S.M.; Abedi, S.; Gharehpetian, G.B.; Hosseinian, S.H.; Abedi, M. Introducing a Novel DC Power Flow Method With Reactive Power Considerations. *IEEE Trans. Power Syst.* **2015**, *30*, 3012–3023. [CrossRef]
26. Liu, D.; Liu, L.; Cheng, H.; Zhang, S.; Xin, J. An Extended DC Power Flow Model Considering Voltage Magnitude. *J. Mod. Power Syst. Clean Energy* **2021**, *9*, 679–683. [CrossRef]
27. Mostafa, M.H.; Aleem, S.H.E.A.; Ali, S.G.; Abdelaziz, A.Y.; Ribeiro, P.F.; Ali, Z.M. Robust Energy Management and Economic Analysis of Microgrids Considering Different Battery Characteristics. *IEEE Access* **2020**, *8*, 54751–54775. [CrossRef]
28. Ebeed, M.; Aleem, S.H.E.A. Chapter 1—Overview of uncertainties in modern power systems: Uncertainty models and methods. In *Uncertainties in Modern Power Systems*; Zobaa, A.F., Abdel Aleem, S.H., Eds.; Academic Press: Cambridge, MA, USA, 2021; pp. 1–34. [CrossRef]
29. Zimmerman, R.D.; Murillo-Sánchez, C.E.; Thomas, R.J. MATPOWER: Steady-State Operations, Planning, and Analysis Tools for Power Systems Research and Education. *IEEE Trans. Power Syst.* **2011**, *26*, 12–19. [CrossRef]